**Preprints of the 19th World Congress**
**The International Federation of Automatic Control**
**Cape Town, South Africa. August 24-29, 2014**

# Model-based supervision of a blood pump

**André Stollenwerk** * **Jan Kühn** * **Christian Brendle** **
**Marian Walter** ** **Jutta Arens** *** **Markus Nabil Wardeh** ****
**Stefan Kowalewski** * **Rüdger Kopp** ****

* *Embedded Software Laboratory*
** *Philips Chair for Medical Information Technology*
*** *Department of Cardiovascular Engineering, Institute of Applied Medical Engineering*
**** *Department of Intensive Care Medicine*
*all with RWTH Aachen University, 52056 Aachen, Germany*
*Corresponding author: e-mail: stollenwerk@embedded.rwth-aachen.de*

**Abstract:** In this paper, we present a novel method to supervise several discrete events and continuous processes causing failures in a blood pump. These are potential hazards which regularly cause problems in intensive care routine. We propose an indicator that considers the nonlinear shear thinning flow properties of blood. Based on a threefold of physiological motivated measures, we calculate an indicator which is not only able to detect ongoing events like gas in the blood phase but also to predict upcoming events like the suction of the withdrawing cannula to the surrounding vessel's wall. We present an algorithm that is embedded in a distributed 32 bit microcontroller network and holding hard real-time constraints. We were able to evaluate out algorithms in-vivo. For this algorithm we analyzed online data of more than 140 hours of animal experiments.

## 1. INTRODUCTION

In intensive care medicine, patients are increasingly treated with extracorporeal organ support using extracorporeal blood circulation (cf. Paden et al. [2013], Cohn [2003]). Insufficient physiological conditions of patients are supported or even temporally replaced utilizing treatment methods outside the human body. In these therapies the focus is often on blood. Either, undesired substances are eliminated (e.g., during dialysis), or needed substances are fed (e.g., oxygen during lung assist). In this manner, the blood circulation itself can be supported via, e.g., a ventricular assist device or a cardiopulmonary bypass.

Blood, which is the medium of interest, adds the difficulty of being a non-Newtonian fluid. The flow properties of blood do not only depend on flow and pressure but also on the varying viscosity. The viscosity of a shear thinning fluid such as blood depends on the shear stress which it is exposed to. There are existing models for calculating the flow properties of blood, but these models need to know the exact geometry of the whole piping system and are generally solved using numerical techniques such as the finite element method (Lou and Yang [1993], Johnston et al. [2006], Nichols and O'Rourke [2011]).

Modeling of the whole extracorporeal circulation in interaction with the human body in detail is still an unresolved problem. Measuring the conduit-structure of each individual setup would be necessary due to the geometric complexity of the cardiovascular system and unavoidable variations in the extracorporeal tubing. Otherwise, the parameterization of the subsidiary fluid dynamical models would not be possible. Therefore, only very small volumes are modeled in detail or approximations are used to describe the behavior.

For the design of a control or safety concept, there is the need of a fluid-dynamical model of the system. Often for simplification, a model with fixed viscosity is used. Particularly for safety measures, this loss of accuracy is not tolerable. Hence, we extended the model of a Newtonian fluid with temporal bounded uncertainties in order to consider the shear thinning properties of blood.

### *1.1 Worked example*

In this work, we focus on a model-based safety concept for a rotary blood pump (diagonal pump). This pump is used as actuator during an extracorporeal lung assist (ECLA) treatment. Here, a failure of the pump would be life threatening. Using supervision of differences between the model and the controlled system, we are able to detect several discrete events like gas bubbles within the transported blood or the suction of the withdrawing cannula to the surrounding vessel, and the continuous wearout of the pump due to the accumulation of blood clots (coagulation). We also investigate on the performance of the derived algorithms. The aim is to be able to embed the algorithms to an embedded safety network of microcontrollers.

## 2. NEWTONIAN FLUID-DYNAMICAL MODEL OF THE BLOOD-PUMP

In general, a rotary blood-pump transfers energy, from the rotation of a motor, to a blood-flow and a pressure difference over the pump, respectively (Karassik et al.

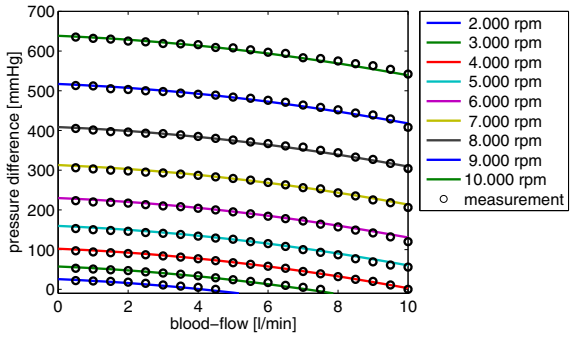


Fig. 1. Parameterized model of the characteristic curve according to equation (1) of a Medos DP2 blood pump

[2001], Reul and Akdis [2000]). For the utilized diagonal-pump – Medos DP2 – the generated pressure difference over the pump transporting a Newtonian fluid can be described as:

$$\Delta p(Q(t), \omega(t)) = \alpha_1 \cdot Q(t) + \alpha_2 \cdot Q(t)^2 + \alpha_3 \cdot \omega(t)^2, \quad (1)$$

where $Q$ is the blood-flow and $\omega$ is the revolution speed of the impeller. The coefficients $\alpha_1$, $\alpha_2$ and $\alpha_3$ can be identified depending on the pump geometry and the transported fluid, especially the viscosity. There are other comparable models presented in literature (Choi et al. [1997], Misgeld [2007]).

All mentioned models have in common that only fixed viscosity fluids are considered; this is not suitable for blood. For closed-loop blood flow controller design, this discrepancy can be neglected if there are no high dynamics, such as pulsatile flow, in the system and the control algorithm has no permanent deviation, e.g., due to an integral term.

In Figure 1, the characteristic curve of the Medos DP2 diagonal blood pump for a water glycerol solution is given for several rotational speeds. This fluid has flow properties comparable to blood (dynamic viscosity of $\eta = 3,6$ mPa at a temperature of 37 °C). Each circle represents a measurement point. The solid lines are generated by a pump specific parameterization of equation (1).

The applicability of the presented model is shown in Figure 2. The plot shows the pressure difference generated over the blood-pump during a porcine animal experiment versus the calculation based on equation (1). In general, a good correlation is shown. In detail, there is a too low predicted pressure difference around 1:00 PM and a too high pressure difference at about 1:15 PM. At 1:10 PM and 1:22 PM, instationarity in the measured pressure difference can be recognized; they are caused by changes in the blood flow and the accompanying change in viscosity. This variation of viscosity is disregarded in the presented model. At large, the error of the model highly depends on the operating point of the blood-pump and can be positive or negative, respectively.

In this section, a well known model for the pressure difference generated by a diagonal blood-pump was presented. The characterization only holds for Newtonian

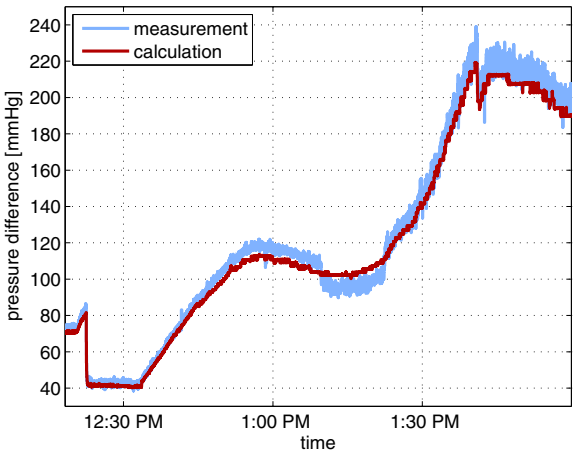


Fig. 2. Preasure difference model and archieved values by the blood pump during an animal experiment

fluids, which yet is sufficient in most cases of blood flow controller design.

## 3. FUZZY MODELING OF THE CONVEING NON-NEWTONIAN FLUIDS

The mathematical model presented in Section 2 only holds for fixed viscosity fluids. Blood is, as already illustrated, a shear thinning fluid. Hence, equation (1) only holds for massively restricted conditions.

In literature, several models for the non-Newtonian blood flow were presented (Lou and Yang [1993], Johnston et al. [2006], Nichols and O'Rourke [2011]). All of them base on the Navier-Stokes equations. Hence, the mathematical modeling could be extended for non-Newtonian fluids. Therefore, the exact geometry of the whole setup needs to be parameterized and one will need exact information about the velocity vector field of the fluid. This class of models is in general only solved using numerical approximations such as CFD (Computational Fluid Dynamics). These models usually are computationally complex. Thus, CFD is used for geometric improvements but neglected for safety supervision.

For the blood pump supervision, an adequate precise but low computational-effort model is needed. In this section, we will present a physiological motivated set of parameters to supervise. These parameters enable the needed fuzziness to take account for the shear thinning properties of blood.

### *3.1 Flow impedance*

In analogy to the electrical impedance, the quotient of pressure difference and blood flow is defined as flow impedance:

$$Z_F(t) = \frac{\Delta p(t)}{Q(t)}. \quad (2)$$

This parameter describes the flow impedance observed by the blood pump. It adds up all tubing, cannulas, the patient and, if existing, any additional extracorporeal treatment devices. Thus, $Z_F$ combines all variations in

rigidity — including compliance of the patient's vessels. During an extracorporeal treatment, varying factors can influence $Z_F$. Hence, it cannot be regarded as constant. We assume that all regular causes of a change in flow impedance have slow dynamics.

This leads to the analysis of the variation of the flow impedance in a time window with a width of 10 seconds. Thereby, we linearize $Z_F$ in the actual operating point of the pump. The flow impedance, as described in equation (2), is derivated and folded with a Hamming window with a width of 10 seconds. In order to emphasize higher variations, this result is squared.

$$\widetilde{Z}'_F(t) = c_1 \cdot \left( w_{\text{Ham,10 s}} * \frac{\mathrm{d}Z_F(t)}{\mathrm{d}t} \right)^2 \tag{3}$$

With this measure $\widetilde{Z}'_F(t)$, the variable physiology of the patient is aggregated, but discrete events to the tubing, e.g., bended tubing, can be determined.

### *3.2 Deviation of pressure model*

In Section 1, we already introduced the varying flow properties of blood. These properties lead to a noticeable chance of a permanent deviation between the measured pressure difference and the model-based calculated one. Therefore, we only consider a lightly weighted squared relative error:

$$E_p(t) = c_2 \cdot \left( \frac{\Delta p_{\text{measured}}(t) - \Delta p_{\text{calculated}}(t)}{\min\left(\Delta p_{\text{measured}}(t), \Delta p_{\text{calculated}}(t)\right)} \right)^2. \tag{4}$$

By squaring the calculated error, we not only avoid negative errors but also award an upcoming error with an increased interest.

### *3.3 Homogeneity of alteration rate*

In contrast to the relative error $E_p$ (cf. Section 3.2), the relative changes within the measured and calculated pressure differences should be comparable. Consequently, an increasing $\Delta p_{\text{measured}}(t)$ should be accompanied by an increasing $\Delta p_{\text{calculated}}(t)$ and vice versa.

As a last measure, the derivation of both pressure differences are compared as a squared difference. In order to consider the transient properties, we use the 10 seconds window again (cf. Section 3.1).

$$E_h(t) = \tag{5}$$
$$c_3 \cdot \left( w_{\text{Ham,10 s}} * \left( \frac{\mathrm{d}\Delta p_{\text{measured}}(t)}{\mathrm{d}t} - \frac{\mathrm{d}\Delta p_{\text{calculated}}(t)}{\mathrm{d}t} \right) \right)^2$$

### *3.4 Resulting indicator*

These three measures as defined in (3), (4) and (5) were combined to a single indicator by weighted summation. As motivated, the deviation of the pressure model to the measurements was taken into account only marginally. The sum is normalized by choosing the constants $c_1$, $c_2$ and $c_3$ in such a way, that an indicator of 1 or more can be regarded as a detected fault. This fault detection threshold is highlighted in each plot as a red dashed line. The normalization and determination of the constants was performed empirically, based on the data of porcine animal experiments. Therefore, we need further investigation on the transferability of the constants to humans.

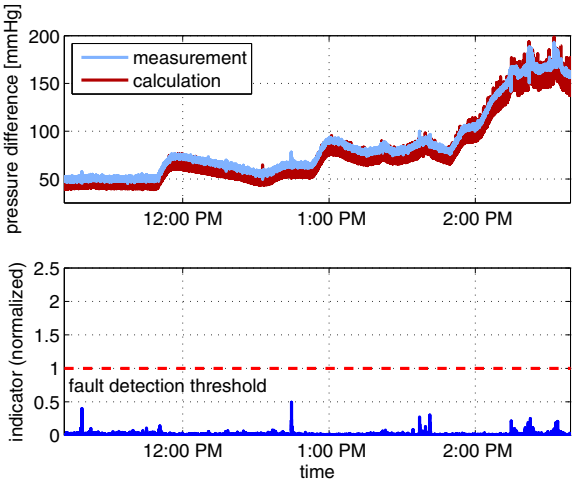


Fig. 3. Exemplary analysis of animal experiment data

An exemplary analysis is shown in Figure 3. The upper diagram shows the measured and the calculated pressure difference (cf. Figure 2). The lower diagram shows the progression of the introduced indicator. One can see peaks of up to 0.5, but during the observed period, no fault occurred, so the indicator stays silent.

## 4. EVALUATION

For evaluation of the proposed indicator, first of all, the model as stated in equation (1) needed to be parameterized. Therefore, we conducted an in-vivo experiment during which the speed of the pump motor was varied. We repeatedly recorded the range from 1000 rpm to 10000 rpm in 10 steps. Additionally, multiple speed jumps (step responses) were traced.

By this original data (28 minutes of measurement), we parameterized the coefficients $\alpha_1$ to $\alpha_3$ in equation (1). The resulting mean error over the calibration is $-11.02$ mmHg with a standard deviation of 24.51 mmHg.

In the following, three representative events are exemplarily shown. In general, we evaluated this indicator against about 140 hours of data, collected during animal experiments conducted with 15 midi-pigs (ø-weight 50 kg, cf. Stollenwerk [2013]). All experiments were conducted according to ethical principles of laboratory animal care (approved by the appropriate governmental animal care committee (LANUV, NRW, Germany)). The animals were treated according to experimental protocol defined in Kopp et al. [2011].

The implementation of the algorithms according to equations (3), (4) and (5) was conducted in MATLAB (Release 2012b, The MathWorks, Natick, MA). Subsequently, these algorithms were cross-complied to C-code in order

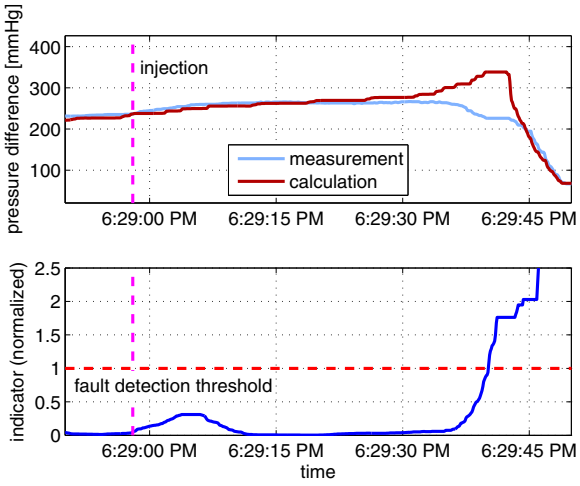


Fig. 4. Injection of 0.5 ml of air in the extracorporeal blood circulation (at a blood flow of 3.3 $^{L}/_{min}$)

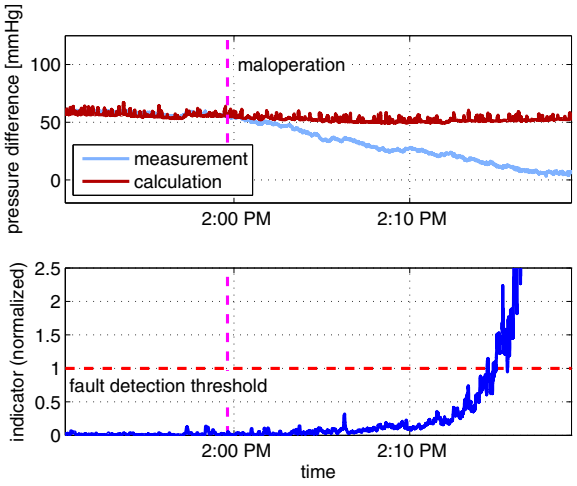


Fig. 5. Failure of the pressure sensor due to incorrect operation (at a blood flow of 1.3 $^{L}/_{min}$)

to embed them to a distributed microcontroller network (cf. Stollenwerk et al. [2011b]).

### *4.1 Event: Gas bubbles in blood tubing*

The first evaluated event was the presence of gas bubbles in the blood tubing. If the volume element containing the gas bubbles would be supplied to the patient, infarctions like stroke or heart attack might be a consequence. Therefore, no matter what the gas bubbles have to be detected and the patient needs to be guarded against the introduction of gas bubbles. In order to simulate such an event, we injected different volumes of air at the withdrawal cannula. This gas volume was transported through the tubing into the blood pump. The corresponding pressure plot is given in Figure 4. The dashed purple line indicates the point in time when the gas was injected (6:28:58 PM). Subsequently the gas bubble needed about 35 seconds to move through the tubing (approx. length 115 cm) until it reaches the pump.

Initially, the injection of gas changes the flow impedance by lowering the density of the transported fluid. This results in a slight raise of the introduced indicator. Nevertheless, this discrepancy does not have the sufficient significance, since it is in the same magnitude as caused by the measurement error and the influence of the non-Newtonian flow properties of blood. When the gas bubbles approach the pump, the perfusion behavior of the pump is changed over all three parameters such that this event can be dependably detected. With gas volumes of a sufficient size, already the injection can be detected. Unfortunately, we only injected volumes between 2.0 ml and 0.5 ml into the circulation. Therefore, we cannot draw a lower bound beneath which injected gas cannot be detected anymore. This is one aspect which should be evaluated in the future.

### *4.2 Event: Sensor failure*

Another addressed problem by the indicator is sensor failure. The measurement plot shown in Figure 5 was falsified by the maloperation of a three-way stopcock. After the withdrawal of a blood gas analysis specimen the cock was not set back to the correct position.

One of the used pressure sensors was connected via this three-way stopcock to the blood tubing system. This cock enables interaction with the tubing, e.g., drawing of blood specimen or delivery of drugs without additional tapping.

Due to the maloperated cock the measured pressure difference trended to a pressure difference of 0 mmHg. By the means of the introduced indicator, this failure could be detected after 15 min; before this behavior could cause any harm to the patient.

### *4.3 Event: Suction of withdrawing cannula*

A last example for a detectable discrete event is shown in Figure 6. During the operation of an extracorporeal circulation, it might occur that the withdrawing cannula sucks too much blood out of the vessel. Then, the tip of the cannula is occluded by the wall of the surrounding vessel. This results in an instantaneously drop of the blood flow. The causing physiological conditions can, e.g., be dehydration of the patient.

Since the only chance to reestablish the extracorporeal circulation after such an event is to shut down and restart the whole circulation, it should be avoided in any case. The discontinuation of the extracorporeal treatment of the patient regularly is accompanied by a serious hazard for the patient's life.

The pressure plot in Figure 6 shows a spontaneous drop at 1:09:30 PM, which is the moment the flow grinded to a halt. Already some 90 seconds prior to the occlusion an abnormal behavior of the pressure signal can be recognized. The introduced indicator exceeds the limit about 50 seconds before the drop of the blood flow, which regularly is sufficient for the intensive care physicians to take the correct actions, e.g. supply saline solution. Anyhow, we were able to develop another model based measure dedicated to cannula occlusion, which is able to predict the drop of the blood flow up to 90 seconds in advance (cf. Stollenwerk et al. [2011a]).

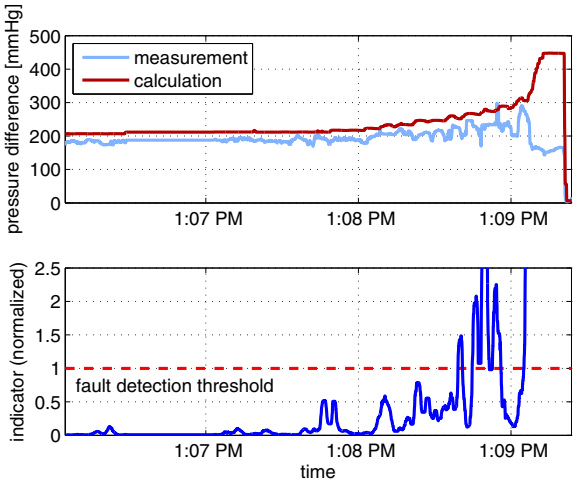


Fig. 6. Suction of the tip of the withdrawal cannula to the surrounding vessel

### *4.4 Continuous processes*

During two of the conducted experiments, mechanical stress within the bearing of the impeller caused significant coagulation. During the experiments, the indicator constantly rose. After the experiments the whole tubing was washed and the clot could visually be validated within the pump.

Since we cannot state anything about the intermediate status of the clot, a direct mapping from the indicator to the clot's size is not possible at this moment. Therefore, we want to establish a model for generating clots of controlled sized and evaluate the phenomenon separated in-vitro. Using this model, we expect to be able to better fit the algorithms to the behavior during clotting and state the detection probabilities for clotting in the blood pump related to clot size, respectively. Nevertheless, the correlation between the risen indicator and clotting in the tubing in general proves the applicability.

Besides bending of the tubing, also leakages can be detected. We lead a part of the blood flow into a reservoir. The leakage resulted in a change of flow impedance, which could be detected in specific cases. Further experiments have to point out the lower bound of the ratio of blood flow to leakage that can be detected with certainty.

### *4.5 Worst-case execution time and real-time properties*

The whole algorithm was run on an ARM7 microcontroller. A formal analysis of the software showed, that one iteration of the algorithm results in a worst-case sum of 6633 cycles. This leads to a CPU time of 0.138 milliseconds on the utilized Atmel AT91SAM7 hardware with a clock speed of 48 MHz. Hence, the presented algorithm is appropriate for application in an embedded hardware environment. Real-time calculation of the indicator can be guaranteed utilizing our hard- and software architecture (cf. Stollenwerk [2013], Stollenwerk et al. [2011b]). The worst-case execution time analysis was conducted using aiT for AMR7 version 11.08 build 166667 from AbsInt (cf. Ferdinand and Heckmann [2004]).

## 5. CONCLUSION

We introduced an indicator that adds a new keystone towards sound operation of extracorporeal circulation. By the application of model-based safety measures, we are able to detect various discrete events such as gas bubbles in the extracorporeal circulation, sensor failure, or cannula suction, as well as continuous processes such as coagulation or leakages. Naturally, these continuous processes can only be addressed after exceeding a certain threshold. This especially holds for the detection of leakage. Very small amounts of lost blood like occasional drops cannot be detected by the measures presented in this paper.

The achievements shown were conducted by fuzzy modeling of the conveying non-Newtonian fluids. In contrast to earlier attempts, we took the sheer thinning properties of blood into account, which enabled us to establish physiological motivated models with higher specificity and sensitivity.

We were able to show the applicability of our model-based indicator by in-vivo experiments with broad base data. Events, regularly causing hazards in clinical routine, like suction of cannula or infarction causing gas bubbles within the blood, could be detected reliably.

## 6. OUTLOOK

With reference to the monitored continuous processes, we are elaborating more fine-grained methods to supervise processes like coagulation within the pump. This shall improve the prediction and modeling of these processes.

In the proposed algorithm, the fuzziness is not dependent of the operating point of the system. We want to investigate whether such a dependency would enable us to increase the specificity of detecting different or even additional hazards.

In Section 4, we were able to show that the introduced indicator is able to detect volumes of down to 0.5 ml of gas within the blood tubing. This evaluation should be extended to even smaller volumes in order to determine a lower bound for which volumes can be detected reliable.

The used constants within the formulae were empirically fitted to 140 hours of porcine experiments. A rule of derivation for these constants should be elaborated based on a broader data base, which should enable the parameterization of other blood pumping devices in addition. This should enable a more general assessment of the indicator and its application. In addition, the transition to human blood properties should be investigated.

An additional metered parameter in the system is the energy consumption of the blood pump. According to the law of conservation of energy, we are able to also consider these parameters. If no improvement of the existing algorithms could be achieved, one should at least be able to additionally monitor the hypovolemia caused by hyperthermia.

## ACKNOWLEDGEMENTS

This work was supported by the German Research Foundation DFG (DFG - Grant PAK 138/2) and by the DFG

Cluster of Excellence on Ultra-high Speed Information and Communication (UMIC), (DFG-Grant EXC 89). The authors gratefully acknowledge this contribution.

## REFERENCES

Seongjin Choi, J. R. Boston, D. Thomas, and J. F. Antaki. Modeling and identification of an axial flow blood pump. In *American Control Conference*, volume 6, pages 3714–3715, 1997.

Lawrence H. Cohn. Fifty years of open-heart surgery. *Circulation*, 107:2168–2170, 2003.

Christian Ferdinand and Reinhold Heckmann. ait: worst case execution time prediction by static program analysis. In *IFIP Congress Topical Sessions*, pages 377–384, 2004.

Barbara M Johnston, Peter R Johnston, Stuart Corney, and David Kilpatrick. Non-newtonian blood flow in human right coronary arteries: transient simulations. *Journal of biomechanics*, 39(6):1116–1128, 2006.

Igor Karassik, Joseph Messina, Cooper Paul, and Charles Heald. *Pump handbook*. McGraw-Hill, New York, 2001.

Ruedger Kopp, Ralf Bensberg, Jutta Arens, Ulrich Steinseifer, Thomas Schmitz-Rode, Rolf Rossaint, and Dietrich Henzler. A miniaturized extracorporeal membrane oxygenator with integrated rotary blood pump: Preclinical in vivo testing. *ASAIO J*, 57(3):158–163, May/June 2011.

Zheng Lou and Wen-Jei Yang. A computer simulation of the non-newtonian blood flow at the aortic bifurcation. *Journal of biomechanics*, 26(1):37–49, 1993.

Berno J. E. Misgeld. *Automatic control of the heart-lung machine*. Dissertation, Ruhr-Universität Bochum, 2007.

Wilmer W Nichols and Michael F O'Rourke. *McDonald's blood flow in arteries: theoretical, experimental, and clinical principles*. CRC Press, 2011.

Matthew L. Paden, Steven A. Conrad, Peter T. Rycus, Ravi R. Thiagarajan, and ELSO Registry . Extracorporeal life support organization registry report 2012. *ASAIO J*, 59(3):202–210, 2013.

Helmut M. Reul and Mustafa Akdis. Blood pumps for circulatory support. *Perfusion*, 15(4):295–311, Jul 2000.

André Stollenwerk. *Ein modellbasiertes Sicherheitskonzept für dieextrakorporale Lungenunterstützung*. Dissertation, RWTH Aachen, July 2013.

André Stollenwerk, Felix Gathmann, Jutta Arens, Ralf Bensberg, Marian Walter, Rüdger Kopp, and Stefan Kowalewski. Safety aware pump-control for a rotary ecmo blood pump. In *The International Journal of Artificial Organs*, volume 34 of *2011*, page 617. Wichtig Editore, August 2011a.

André Stollenwerk, Florian Göbe, Marian Walter, Tobias Wartzek, Rüdger Kopp, Jutta Arens, and Stefan Kowalewski. Smart data provisioning for model-based generated code in an intensive care application. In *High Confidence Medical Devices, Software, and Systems & Medical Device Plug-and-Play Interoperability (HCMDSS/MDPnP 2011), Chicago, USA*, 2011b.